Versailles Project on Advanced Materials and Standards interlaboratory study on intensity calibration for x-ray photoelectron spectroscopy instruments using low-density polyethylene

Benjamen P. Reed,[1,a)] David J. H. Cant,[1] Steve J. Spencer,[1] Abraham Jorge Carmona-Carmona,[2] Adam Bushell,[3] Alberto Herrera-Gómez,[2] Akira Kurokawa,[4] Andreas Thissen,[5] Andrew G. Thomas,[6] Andrew J. Britton,[7] Andrzej Bernasik,[8] Anne Fuchs,[9] Arthur P. Baddorf,[10] Bernd Bock,[11] Bill Theilacker,[12] Bin Cheng,[13] David G. Castner,[14] David J. Morgan,[15] David Valley,[16] Elizabeth A. Willneff,[17] Emily F. Smith,[18] Emmanuel Nolot,[19] Fangyan Xie,[20] Gilad Zorn,[21] Graham C. Smith,[22] Hideyuki Yasufuku,[23] Jeffery L. Fenton,[24] Jian Chen,[20] Jonathan D. P. Counsell,[25] Jörg Radnik,[26] Karen J. Gaskell,[27] Kateryna Artyushkova,[16] Li Yang,[28] Lulu Zhang,[4] Makiho Eguchi,[29] Marc Walker,[30] Mariusz Hajdyła,[8] Mateusz M. Marzec,[8] Matthew R. Linford,[31] Naoyoshi Kubota,[29] Orlando Cortazar-Martínez,[2] Paul Dietrich,[5] Riki Satoh,[29] Sven L. M. Schroeder,[7] Tahereh G. Avval,[31] Takaharu Nagatomi,[32] Vincent Fernandez,[33] Wayne Lake,[34] Yasushi Azuma,[4] Yusuke Yoshikawa,[35,b)] and Alexander G. Shard[1]

AFFILIATIONS

[1]National Physical Laboratory, Hampton Road, Teddington TW11 0LW, United Kingdom
[2]CINVESTAV-Unidad Queretaro, Queretaro 76230, Mexico
[3]Thermo Fisher Scientific (Surface Analysis), East Grinstead RH19 1XZ, United Kingdom
[4]National Metrology Institute of Japan (NMIJ), National Institute of Advanced Industrial Science and Technology (AIST), 1-1-1 Higashi, Tsukuba, Ibaraki 305-8565, Japan
[5]SPECS Surface Nano Analysis GmbH, Voltastraße 5, 13355 Berlin, Germany
[6]School of Materials, Photon Science Institute and Sir Henry Royce Institute, Alan Turing Building, University of Manchester, Oxford Road, Manchester M13 9PL, United Kingdom
[7]Versatile X-ray Spectroscopy Facility, School of Chemical and Process Engineering, University of Leeds, Leeds LS2 9JT, United Kingdom
[8]Academic Centre for Materials and Nanotechnology, AGH University of Science and Technology, 30-059 Kraków, Poland
[9]Robert Bosch GmbH, Robert-Bosch-Campus, 71272 Renningen, Germany
[10]Center for Nanophase Materials Sciences, Oak Ridge National Laboratory, 1 Bethel Valley Road, Oak Ridge, Tennessee 37830
[11]Tascon GmbH, Mendelstr. 17, D-48149 Münster, Germany
[12]Medtronic, 710 Medtronic Parkway, LT240, Fridley, Minnesota 55432
[13]Analysis and Testing Center, Beijing University of Chemical Technology, Beijing 100029, People's Republic of China
[14]National ESCA and Surface Analysis Center for Biomedical Problems, Department of Bioengineering and Chemical Engineering, University of Washington, Seattle, Washington 98195
[15]Cardiff Catalysis Institute, School of Chemistry, Cardiff University, Main Building, Cardiff CF10 3AT, United Kingdom
[16]Physical Electronics Inc., East Chanhassen, Minnesota 55317
[17]Versatile X-ray Spectroscopy Facility, School of Design, University of Leeds, Leeds LS2 9JT, United Kingdom
[18]Nanoscale and Microscale Research Centre, University of Nottingham, Nottingham NG7 2RD, United Kingdom
[19]CEA-LETI, 17 rue des Martyrs, 38054 Grenoble, France

[20]Instrumental Analysis & Research Center, Sun Yat-sen University, Guangzhou 510275, People's Republic of China [21]GE Research, 1 Research Circle, K1 1D7A, Niskayuna, New York 12309
[22]Faculty of Science and Engineering, University of Chester, Thornton Science Park, Chester CH2 4NU, United Kingdom
[23]Materials Analysis Station, National Institute for Materials Science (NIMS), 1-2-1 Sengen, Tsukuba, Ibaraki 305-0044, Japan
[24]Medtronic, 6700 Shingle Creek Parkway, Brooklyn Center, Minnesota 55430
[25]Kratos Analytical Ltd., Wharfside, Trafford Wharf Road, Manchester M17 1GP, United Kingdom
[26]Bundesanstalt für Materialforschung und -prüfung (BAM), Unter den Eichen 44-46, 12203 Berlin, Germany
[27]Department of Chemistry and Biochemistry, University of Maryland, College Park, Maryland 20742
[28]Department of Chemistry, Xi'an Jiaotong-Liverpool University, 111 Ren'ai Road, Suzhou Dushu Lake Science and Education Innovation District, Suzhou Industrial Park, Suzhou 215123, People's Republic of China
[29]Analysis Department, Materials Characterization Division, Futtsu Unit, Nippon Steel Technology Co. Ltd., 20-1 Shintomi, Futtsu City, Chiba 293-0011, Japan
[30]Department of Physics, University of Warwick, Coventry, West Midlands CV4 7AL, United Kingdom
[31]Department of Chemistry and Biochemistry, Brigham Young University, C100 BNSN, Provo, Utah 84602
[32]Platform Laboratory for Science and Technology, Asahi Kasei Corporation, 2-1 Samejima, Fuji, Shizuoka 416-8501, Japan
[33]Université de Nantes, CNRS, Institut des Matériaux Jean Rouxel, IMN, F-44000 Nantes, France
[34]Atomic Weapons Establishment (AWE), Aldermaston, Reading, Berkshire RG7 4PR, United Kingdom
[35]Material Analysis Department, Yazaki Research and Technology Center, Yazaki Corporation, 1500 Mishuku, Susono-city, Shizuoka 410-1194, Japan

Note: This paper is part of the Special Topic Collection on Reproducibility Challenges and Solutions.
[a)]Author to whom correspondence should be addressed: benjamen.reed@npl.co.uk
[b)]Present address: Technical & Project Support Department, Nidec Sankyo CMI Corporation, 46-1, Senpuku, Susono-city, Shizuoka 460-1116, Japan

ABSTRACT

We report the results of a Versailles Project on Advanced Materials and Standards interlaboratory study on the intensity scale calibration of x-ray photoelectron spectrometers using low-density polyethylene (LDPE) as an alternative material to gold, silver, and copper. An improved set of LDPE reference spectra, corrected for different instrument geometries using a quartz-monochromated Al Kα x-ray source, was developed using data provided by participants in this study. Using these new reference spectra, a transmission function was calculated for each dataset that participants provided. When compared to a similar calibration procedure using the NPL reference spectra for gold, the LDPE intensity calibration method achieves an absolute offset of ∼3.0% and a systematic deviation of ±6.5% on average across all participants. For spectra recorded at high pass energies (≥90 eV), values of absolute offset and systematic deviation are ∼5.8% and ±5.7%, respectively, whereas for spectra collected at lower pass energies (<90 eV), values of absolute offset and systematic deviation are ∼4.9% and ±8.8%, respectively; low pass energy spectra perform worse than the global average, in terms of systematic deviations, due to diminished count rates and signal-to-noise ratio. Differences in absolute offset are attributed to the surface roughness of the LDPE induced by sample preparation. We further assess the usability of LDPE as a secondary reference material and comment on its performance in the presence of issues such as variable dark noise, x-ray warm up times, inaccuracy at low count rates, and underlying spectrometer problems. In response to participant feedback and the results of the study, we provide an updated LDPE intensity calibration protocol to address the issues highlighted in the interlaboratory study. We also comment on the lack of implementation of a consistent and traceable intensity calibration method across the community of x-ray photoelectron spectroscopy (XPS) users and, therefore, propose a route to achieving this with the assistance of instrument manufacturers, metrology laboratories, and experts leading to an international standard for XPS intensity scale calibration.

I. INTRODUCTION

X-ray photoelectron spectroscopy (XPS) is a highly surface sensitive technique that can determine the elemental composition and chemical environment of the top few nanometers (∼10 nm) of a material's surface. XPS has become synonymous with surface analysis, with many industries and academic institutes regularly using quantitative XPS in their research, especially as it becomes more accessible through commercial XPS instruments.[1] Quantitative XPS analysis relies on the extraction of accurate peak intensities (i.e., their area) from measured spectra in order to ascertain the concentration of specific elements and chemical species in the sample. The intensity, I_n, of a photoelectron peak for a given

element, n, is affected by both physical factors and experimental factors such that, for a homogeneous material,

$$I_n \doteq N_n J \lambda_E F \frac{\sigma}{4\pi} T, \quad (1)$$

where N_n is the atomic concentration of element n, J is the x-ray flux incident on the sample, λ_E is the energy-dependent inelastic mean free path,[2] F is a term related to the photoelectron angular emission distribution and analyzer geometry,[3] σ is the core level photoionization cross section,[4,5] and T is the transmission efficiency of photoelectrons through the analyzer as a function of kinetic energy, commonly called the "transmission function." Except for N_n (assuming it is unknown) and T, all these factors can be estimated through theoretical calculations, found in lookup tables, or factored out when comparing relative intensities acquired using the same experimental parameters. As with all experimental apparatus, XPS instruments require regular calibration. The intensity scale of an XPS instrument is calibrated by determining the T of the analyzer, which is affected by the detector efficiency and factors such as the overlap between the x-ray spot and the collection area of the analyzer for a given sample positioning and orientation (usually, the position of the sample is chosen to maximize counts; the calibration is usually done with the sample facing the analyzer). T is also affected by analyzer settings such as the pass energy, defined sample analysis area, slit/iris settings, voltage across the microchannel plate, and the operating mode of the electromagnetic lens stack, to name a few. A unique transmission function should be determined for all regularly used combinations of analyzer settings to ensure consistency across multiple experiments. The transmission function will drift over time and when a significant change is made to the XPS instrument (e.g., after a bakeout), so without regular intensity calibration, the accuracy of analyses from a given spectrometer can become unreliable. This issue is compounded when comparing results from different laboratories—if these laboratories do not calibrate their analyzers regularly, or are calibrating with respect to different reference spectra, then comparing XPS data between laboratories will not be possible. In an era where the reproducibility of results in scientific publications is being called into question,[6-8] it seems appropriate to highlight the calibration of the instruments that generate scientific data. Several successful international standards have already been published under the auspices of ISO/TC201/SC7 Electron Spectroscopy Standards. For example, there already exists an international standard for the calibration of energy scales in XPS (ISO 15472:2010),[9] as well as the repeatability and constancy of the intensity scale (ISO 24237:2005).[10] As of writing, there is no international standard protocol for calibrating the intensity scale of XPS spectrometers, and this study is intended to both motivate and inform the generation of such standards. Many methods of intensity calibration and reference materials have been used for XPS instruments,[11-18] including the use of peak intensities,[13,14,18] sample bias,[14] elastic electron scattering from an isotropic electron gun,[15] and general assumptions regarding the transmission of the analyzer, to name a few.[16,17] An intensity calibration method developed at NPL by Seah and Smith compares experimental survey scans from copper, silver, and gold to accurate reference spectra suitable for the instrument geometry.[19-21] The ratio of the experimental result to the accurate reference spectra provides a representation of T with additional experimental noise, denoted as Q. The rapidly changing intensities near the peaks are excluded for two reasons. First, due to differences in instrument resolution, the widths and shapes cannot easily be adapted to provide a suitable match. Second, the large intensities at the peak are more likely to be in error due to detector saturation. An alternative method of determining a spectrometer's transmission function uses low-density polyethylene [LDPE $(C_2H_4)_n$] as a secondary reference material (i.e., where the secondary reference spectrum is obtained from a spectrometer calibrated using a primary reference material such as gold, silver, and/or copper).[22] LDPE is a thermoplastic widely used for containers, packaging, and tubing due to its excellent chemical resistance, flexibility, and toughness, as well as being nontoxic. If measured using XPS without preparation, LDPE will exhibit an O 1s peak on the surface due to long-term environmental oxidation and oxygenated functional groups in adventitious carbon contamination. Previous studies with argon cluster ion sputtering show that this oxidation extends hundreds of nanometers into the material.[22] It was confirmed that scraping an LDPE surface several times with a clean scalpel blade results in an oxygen-free surface that is insensitive to carbon contamination,[23] meaning that LDPE can be prepared ex situ without the need for an ion source for sputtering. LDPE's chemical structure results in a spectrum that contains only carbon-related peaks (i.e., C KLL Auger feature, the C 1s core level, and valence states), with most of the measured photoelectron intensity comprising of inelastic background. The simplicity of the inelastic background means that it can be described by a relatively straightforward mathematical function. This mathematical description of the LDPE inelastic background is easily reproduced, continuous, and noise-free, which is a significant advantage over precious metal reference spectra using this calibration approach.

Under the auspices of Technical Working Area 2 (Surface Chemical Analysis) of the Versailles Project on Advanced Materials and Standards (VAMAS) organization, an interlaboratory study was conducted to further investigate XPS intensity calibration using LDPE as a reference material. The general aim of the study was to assess the validity of this calibration method across a wide range of laboratories with different XPS instruments. To date, this intensity calibration method has only been applied to XPS spectrometers that use a quartz-monochromated Al Kα x-ray source. We did not receive any datasets from participants with nonmonochromated x-ray sources or other anode targets such as Mg or Cr.

II. VAMAS PROJECT A27

A. Experiment

A 150 × 150 × 1 mm^3 sheet LDPE (CAS No. 9002-88-4) was purchased from Goodfellow Cambridge Ltd. (Huntingdon, UK) and cut into 50 individual pieces of ~10 × 20 mm^2 in size. The edges of the LDPE were trimmed with a clean scalpel to remove any ragged edges. Each piece of LDPE was then wrapped in aluminum foil to prevent degradation due to light until the sample was ready to be analyzed by the participant. Two sheets of gold (AU153709, 99.99 % purity, 50 × 50 × 0.125 mm^3) were purchased from Advent Research Materials (Oxford, UK) and cut into 50 individual pieces of ~10 × 10 mm^2 in size. A plastic protective

coating was attached to one side of each gold piece, which was removed using tweezers. Each piece of gold was cleaned by sonication in acetone for 15 min and then sonication in isopropanol for 15 min, followed by blow-drying with argon gas. Clean and sterile disposable scalpels (10A, Ref 0502) were procured from Swann-Morton Ltd. (Sheffield, UK). The samples of LDPE and gold were placed into clean 1 in. Fluoroware wafer shipping containers (Megatech Limited, Huntington, UK). The samples were shipped to the participants along with a disposable scalpel and a hard copy of the protocol (see supplementary material S1).[29]

Participants were asked to mount the LDPE and gold samples onto their instrument's sample holder using any appropriate method. To prepare a fresh oxygen-free surface on the LDPE, participants were required to use the disposable scalpel to scrape the LDPE surface several times until it turned from shiny to matte in appearance. Participants were instructed to ensure that the direction of the last few scrapes were parallel to the x-ray source-analyzer plane to reduce x-ray shadowing effects from the topography generated on the LDPE during preparation. Participants were advised to prepare the LDPE surface immediately before introduction to UHV. If the procedure was performed correctly, then the O 1s signal in XPS should be below the detection limit, which is less than 0.03 at. %.[23] Similarly, the gold surface must also be contaminant-free, so participants were recommended to use in situ Ar-ion sputtering. If they did not have an argon-ion sputtering gun, then they were asked to clean the gold surface using any method available in their laboratory or to evaporate gold in situ. Again, all details on handling of samples can be found in the full protocol in the supplementary material (see S1)[29] or online.[24]

B. Analysis

Prior to any analysis on the samples, participants were instructed to obtain an XPS survey spectrum without a sample in the analysis position and with the x-ray source switched off in order to obtain the "dark noise" count of the XPS instrument. Participants were then asked to switch on their x-ray source and allow at least 30 min for the instrument to equilibrate. On the LDPE, participants were directed to select an area of analysis that was free of oxygen or any other contaminating species. If they were unable to find a clean area, then the LDPE should be scraped with the disposable scalpel again to generate a clean surface. LDPE is naturally insulating so participants were asked to use a low-energy electron source to compensate for surface charging, such that a single-component C 1s peak was observed between 1200 and 1206 eV kinetic energy (for Al Kα x-ray sources). Once the sample height and charge compensation settings were optimized, participants were then instructed to acquire three spectra on the LDPE: an initial full range survey, $I_{initial}$ (180-1500 eV); a high kinetic energy (HKE) region spectrum, I_{HKE} (1195-1500 eV); and a final full range survey, I_{final} (180-1500 eV). The inelastic background in the HKE region of an LDPE spectrum has a low intensity compared to the rest of the spectrum. Participants were, therefore, asked to increase the acquisition time of I_{HKE} by a factor of ~30 to 40 by increasing the dwell time or by taking multiple acquisitions. This procedure was to be repeated on a fresh area of LDPE for each lens mode, pass energy, and slit combination. Participants were free to submit as many datasets for different analyzer parameters as they wished. The minimum requirement was to submit at least one set of spectra acquired using a high pass energy (e.g., ≥90 eV) and a fully open entrance slit. For every set of analyzer parameters used to acquire LDPE spectra, participants were also instructed to acquire a full survey spectrum (180-1500 eV) of sputter-cleaned gold using the same acquisition parameters as the full LDPE survey spectra. The full procedure for acquiring XPS spectra for the inter-laboratory study is described in the protocol in the supplementary material (see S1).[29] A copy can also be obtained from the NPL website.[24]

All spectra were to be exported without any existing transmission function correction and the photoelectron intensity had to be reported in counts per second. Participants were provided with an MS Excel file with which to report their data and metadata back to NPL. This Excel file also provided a step-by-step procedure of how to generate a transmission function from LDPE, and participants were encouraged to attempt the analysis detailed in S1 themselves, although this was not a necessity.[29]

C. Participants

Sample packages were distributed to 44 participating laboratories: 17 academic institutions, 16 industry partners (including 5 XPS instrument manufacturers), and 11 national facilities. At the conclusion of the study, 35 participants returned at least one dataset to NPL. Some participants provided multiple datasets for different instruments and operating conditions. Table I shows a list of participant codes with the corresponding details and geometry of their XPS instruments. A wide variety of instruments from different manufacturers with different geometries allowed the applicability of the LDPE intensity calibration technique to be investigated thoroughly.

III. RESULTS AND DISCUSSION

For each participant and analyzer settings, the set of LDPE spectra, $I_{initial}$, I_{HKE}, and I_{final}, were combined into a single spectrum in counts per second and then a dark noise correction, D, was subtracted. The combined spectrum for a given participant is denoted as I_{PE} herein. Equation (4) in Sec. IV describes how I_{PE} is calculated. The corresponding sputter-cleaned gold spectrum, acquired using the same acquisition parameters, is denoted as I_{Au}. Each participant's I_{PE} (and I_{Au}) was visually checked for any sign of contamination and for evidence of internal scattering in the analyzer; factors in the participants' data that may affect the final transmission function were noted in Table S2 in the supplementary material.[29] By dividing I_{PE} by the LDPE reference spectrum, a noisy representation of the XPS instrument's intensity response, Q, is obtained, from which the instrument's transmission function, T, can be determined. However, this is not the full story.

A. Geometry-corrected reference spectra for polyethylene

In the original publication[22] and VAMAS protocol[24] (S1),[29] the reference LDPE spectrum used for intensity calibration is

TABLE I. List of participants' instruments with corresponding geometry. The terms a, b, and G are detailed in Sec. III and Ref. 26. Where angle b is not reported (—), an angle of 180° has been used to calculate G.

Code	Spectrometer manufacturer/model	Angle a	Angle b	G (2 s.f.)
AA	Thermo Scientific/Alpha 110	41	180	−0.52
AB	Kratos Analytical/Nova	54.7	180	−0.22
AC	PHI/VersaProbe II	45	180	−0.43
AD	Thermo Scientific/Theta 300	56	45	−0.11
AE	PHI/VersaProbe II	45	180	−0.43
AF	Kratos Analytical/Axis Ultra DLD	60	180	−0.10
AG	Thermo Scientific/Nexsa	60	180	−0.10
AH	PHI/VersaProbe II	45	180	−0.43
AI	Scienta Omicron/UHV System	54.7	—	—
AJ	ULVAC-PHI/Quantum 2000	45	180	−0.43
AK	SPECS/PHOIBOS 150	54	180	−0.23
AL	PHI/VersaProbe II	45	180	−0.43
AM	Kratos Analytical/Axis 165	54	180	−0.23
AN	SPECS/PHOIBOS 150	55	180	−0.21
AO	Kratos Analytical/Axis Ultra DLD	60	180	−0.10
AP	Kratos Analytical/Axis Ultra DLD	60	180	−0.10
AQ	Thermo Scientific/VG ESCALAB 250 Xi	58	180	−0.14
AR	PHI/VersaProbe III	45	180	−0.43
AS	Kratos Analytical/Axis Ultra DLD	60	180	−0.10
AT	SPECS/PHOIBOS 150	55	180	−0.21
AU	PHI/Quantera II Hybrid	45	180	−0.43
AV	Surf Sci/SSX-100	75.5	120	0.37
AW	Kratos Analytical/Axis Supra DLD	60	180	−0.10
AX	SPECS/PHOIBOS 150	55	180	−0.21
AY	ULVAC-PHI/Quantera SXM	45	180	−0.43
AZ	Thermo Scientific/Nexsa	60	180	−0.10
AZ	Thermo Scientific/VG ESCALab 250Xi	58	180	−0.14
BA	Kratos Analytical/Axis Supra	60	180	−0.10
BB	PHI/Quantera Hybrid	45	—	—
BC	ULVAC-PHI/Quantera SXM	45	180	−0.43
BD	SSI/S-Probe	55	—	—
BE	Kratos Analytical/Axis Ultra DLD	60	180	−0.10
BF	Thermo Scientific/ESCALAB Xi+	58	180	−0.14
BG	Thermo Scientific/VG ESCALAB 220i-XL	54.7	180	−0.22
BG	ULVAC-PHI/ESCA 5800	60	54.7	0.01
BH	Kratos Analytical/Axis Ultra DLD	60	180	−0.10
BI	Kratos Analytical/Axis Ultra DLD	60	180	−0.10

generated using a six-component mathematical description, which accounts for all of the observed features in the LDPE background. The fitting parameters used to reproduce the LDPE reference spectrum were determined by fitting an NPL transmission function-corrected LDPE spectrum acquired using the NPL spectrometer (Kratos Axis Ultra DLD). The resulting fitting parameters and background description accurately described the measured LDPE spectrum with a systematic error within 1% across most of the spectrum increasing to 5% around the region of the C KLL features. However, these fitting parameters are only valid for instruments with a similar geometry to the NPL spectrometer where the angle between the incoming x-ray vector and the sample-to-analyzer vector, a, is 60°, and the angle between the anode-monochromator-sample plane and analyzer-sample-monochromator plane, b, is 180°. For this work, the geometry of a given instrument is termed [a, b], so the NPL spectrometer has a geometry of [a, b] = [60°, 180°]. As evident in Table I, a variety of instrument geometries were provided, so it was necessary to investigate the effects of instrument geometry on the LDPE spectrum. This is because Al Kα x-rays that interact with a quartz crystal monochromator have some degree of partial polarization, which alters the distribution of photoelectrons as a function of the instrument geometry.[25] A new mathematical description of the LDPE reference spectrum for all geometries has been developed and disseminated by Shard and Reed.[26] It uses a practical form of the angular distribution of photoelectron emission due to partially polarized x-rays and angular anisotropy in photoemission, G, and the

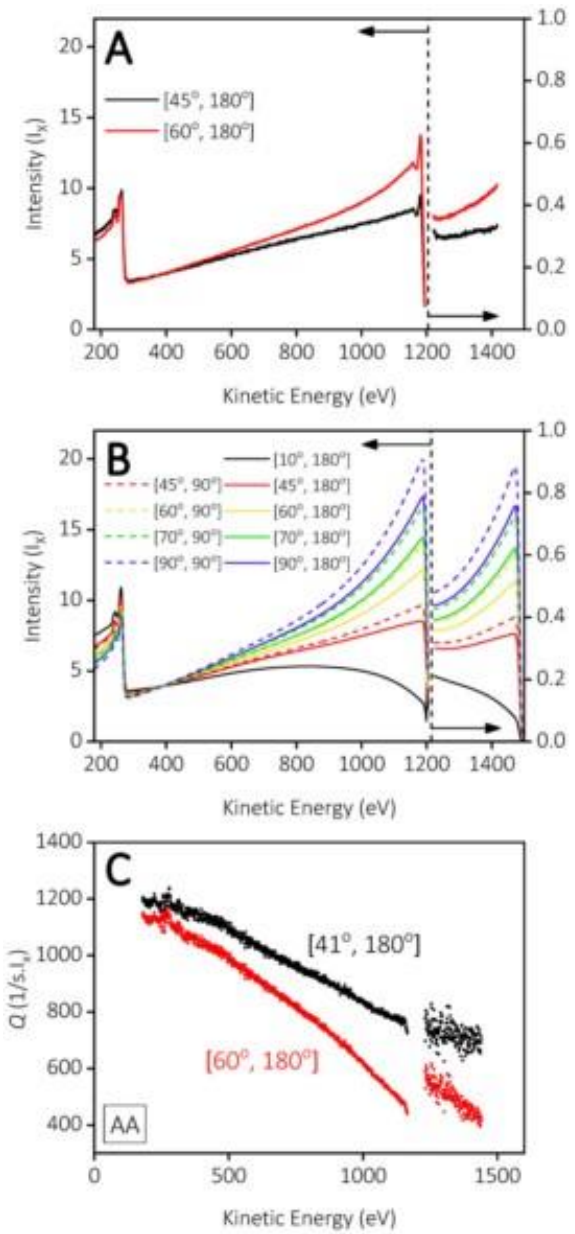

FIG. 1. Geometry correction to the LDPE I_{ref}. In panels (a) and (b), the vertical dashed line denotes an axis break in kinetic energy where the low KE region scale is on the left and the high KE region scale is on the right. (a) The two calibrated LDPE spectra from the VAMAS participants' data. The [45°, 180°] spectrum (black) has lower count rate compared to the [60°, 180°] spectrum (red) across all energies (except for energies less 400 eV). (b) Geometry-corrected LDPE I_{ref} calculated using the method described by Shard and Reed (Ref. 26). A reference spectrum for any combination of a and b can be calculated. (c) The effect of using the new geometry correction on Q_{PE} for participant AA. The lower intensity dots (red) with a large intensity mismatch at ~1200 eV show QPE when calculated using a LDPE Iref for the [60°, 180°] geometry. The high intensity dots (black) without an intensity mismatch show the values of QPE when the correct [41°, 180°] geometry LDPE Iref is used.

energy-dependent geometry correction for elastic scattering, f. Herein, the LDPE reference spectrum for a specific instrument geometry is denoted as I_{ref}. As shown in Table I, the most common geometries encountered during the VAMAS study were [45°, 180°] and [60°, 180°] for which G = −0.43 and −0.10, respectively. Suitable contaminant-free I_{PE} and I_{Au} were selected from the participants that had instrument geometries of [45°, 180°] and [60°, 180°]. The I_{PE} spectra were intensity calibrated using a transmission function determined using their corresponding I_{Au} and the NPL reference spectra for gold. Then, an average intensity-calibrated I_{PE} with intensity units I_X (consistent with the NPL calibration method) was determined for each geometry. Using these averaged spectra, shown in Fig. 1(a), and the methodology described by Shard and Reed,[26] I_{ref} can be determined for any [a, b] instrument geometry. Figure 1(b) shows I_{ref} for varying angles of a and b. Figure 1(c) demonstrates why this geometry correction is required: when I_{PE} from participant AA is divided by the original LDPE reference spectrum described by Shard and Spencer,[22] a significant intensity difference is observed between the high and low kinetic energy sides of the C 1s region. This is because the original LDPE reference spectrum is only valid for an instrument geometry of [60°,180°], and the background intensity dependence on either side of the C 1s region does not match the I_{PE} from participant AA. Using an I_{ref} that is geometry corrected for [41°, 180°], the resulting ratio $Q = I_{PE}/I_{ref}$ does not exhibit the intensity difference around the C 1s region and, therefore, a more sensible description of the spectrometer's transmission function is obtained.

Figure 2(a) shows examples of I_{PE} from several participants. For the purposes of data visualization, these spectra have been normalized to the intensity of the C KLL feature, $I_{C\text{-}KLL}$, in order to compare the inelastic background intensities on the same scale. The corresponding sputter-cleaned gold spectra, I_{Au} (also normalized to the Au NNV area, $I_{Au\text{-}NNV}$, for comparison), acquired using the same analyzer and acquisition parameters are shown in Fig. 2(b). The significant variability of background shapes and intensities of I_{PE} and I_{Au} between different participants visually demonstrates how variable the responses of different instruments are and, therefore, how important the transmission function correction is. I_{PE} was then divided by the corresponding I_{ref} to provide a representation of the transmission function Q. Excluding the regions around the C 1s peak and valence band, the values of Q can then be fitted using the same functional form used in the protocol [see Eq. (3) in Ref. 22] in order to determine a noise-free description of the transmission function T. The values of Q and the functions representing T, shown in Figs. 2(c) and 2(d), are calculated using I_{PE} and I_{Au} shown in Figs. 2(a) and 2(b), respectively. Herein, for each dataset from every participant, the values of Q determined from I_{PE} and I_{Au} are denoted as Q_{PE} and Q_{Au}, respectively. Similarly, the functions of T determined from I_{PE} and I_{Au} are T_{PE} and T_{Au}, respectively. The discrepancies between T_{PE} and T_{Au} for a given participant are discussed later in this report. Once T has been determined for a given set of analyzer parameters, then any spectrum acquired using the same parameters can be intensity corrected using the same T. Figures 2(e) and 2(f) show the initial I_{PE} and I_{Au} divided by their respective T. As expected in the case of the LDPE spectra, the intensity-corrected spectra take on the shape and the intensity of I_{ref}. Participants AX, AT, and AI acquired I_{PE} using the same [55°, 180°] geometry, but the shape and intensity of

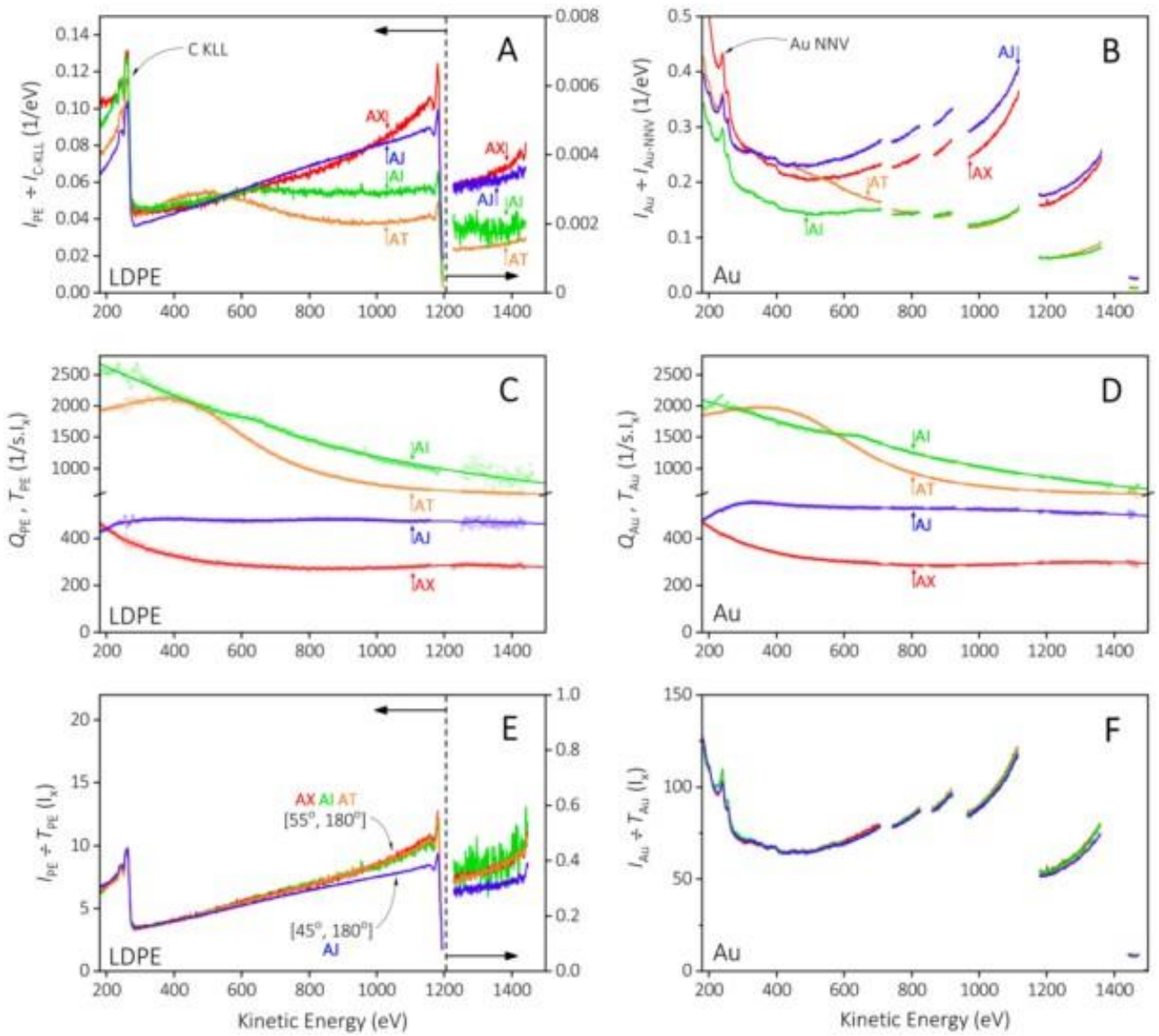

FIG. 2. Examples of transmission function correction using LDPE and Au spectra from participants AX, AJ, AI, and AT. (a) and (b) LDPE and Au spectra normalized to the C KLL and Au NNV Auger peaks, respectively. (c) and (d) Q (dots) and T (lines) calculated using LDPE and Au intensity calibration methods, respectively. (e) and (f) Intensity-corrected LDPE and Au spectra using T_{PE} and T_{Au}, respectively.

the spectra across the kinetic energy range vary significantly. After intensity-correction using their corresponding instrument's T_{PE}, all the LDPE spectra acquired using the [55°, 180°] geometry are identical. Similarly, after intensity-correction using T_{Au}, all the gold spectra exhibit nearly identical shapes and intensities; the relative effect of instrument geometry is less pronounced due to the larger average intensity of gold compared to LDPE. Figures 2(e) and 2(f) demonstrate that the LDPE method of calibration can reach the same result as the NPL intensity calibration method using gold (plus silver and copper) reference spectra. Quantitative analysis of the same sample across these XPS instruments would provide consistent results in terms of peak intensities now that they have functions of T that are traceable to the same set of reference spectra. The values of T are valid for as long as the analyzer is stable (i.e., the transmission function may drift over time as the analyzer ages), and no major changes take place in the XPS instrument (e.g., venting, bakeout, maintenance on components of the XPS instrument, etc.).

B. Analysis of VAMAS data

As discussed previously,[22] the use of the original LDPE reference spectrum for intensity calibration resulted in transmission functions with absolute values within 10% of those calculated using the NPL software and systematic deviations of less than 5%. However, error analysis was only performed on one dataset from the NPL spectrometer with a [60°, 180°] geometry. In line with the aims of VAMAS study A27, the applicability of the LDPE intensity calibration method depends on how this error varies from instrument to instrument and when different analyzer settings are used. T_{Au} is directly traceable to the NPL gold reference spectrum and so, assuming that the gold foil was sputter cleaned correctly and the spectra did not exhibit any scattering or nonlinearity effects, T_{Au} can be used to assess any absolute offset and systematic deviations in T_{PE}. There are limitations to this assessment, which will be discussed later, but it can at least show whether the LDPE intensity calibration method reaches a similar transmission function as gold. The error ratio, R_i, is equal to T_{PE} divided by T_{Au} at kinetic energy data point i. If T_{PE} has the exact same intensity of T_{Au}, then R_i will be equal to unity across all kinetic energies. In practice, R_i deviates from unity across all energies in all the participants' datasets, so it helps define terms that characterize these deviations. The average offset factor, Δ, of T_{PE} with respect to T_{Au} can be determined by subtracting unity from the mean value of the error ratio, R, over all values of i up to the number of kinetic energy data points, n, that is

$$\Delta = \left[\frac{1}{n}\sum_{i=1}^{n} R_i\right] - 1 = [R] - 1. \quad (2)$$

The systematic deviation, Σ, which characterizes the difference in the shape of T_{PE} with respect to T_{Au} is calculated as twice the standard deviation of R_i across all values of i, i.e., $2\sigma_R$, divided by R, such that

$$\Sigma = \frac{2\sigma_R}{R}. \quad (3)$$

The confidence interval of Σ, based on an interval of ±2σ, is 95%, which is enough given that the accuracy of quantification for photoelectron peaks is further limited by errors in the inelastic background selection and effective attenuation length. For clarity, a graphical representation of R_i, Δ, and Σ from participant AM is shown in the supplementary material (Fig. S7).[29] In this work, we calculated the average and standard deviation of R_i over a range of 180-1500 eV kinetic energy. The values of Δ and Σ are relative uncertainties, and so percentage values are obtained by multiplying them by 100. The percentage values of Δ (%) and Σ (%) for each dataset provided by the participants are plotted against each other in Fig. 3. The black dashed lines in Fig. 3 show the mean value of Δ (%) and Σ (%) when considering all the participants' data, which correspond to values of 3.0% and ±6.5%, respectively (1 d.p.). Comparing the datasets with respect to parameters such as lens modes, slit width, and certain other instrumental factors is not possible as the design and operation of each participant's analyzer is not necessarily comparable. However, the analyzer pass energy is a measurable numerical parameter and has a predictable effect on the participants' data, i.e., generally the larger the pass energy, the larger the intensity measured on the detector. The reported pass energies from the participants are separated into one of two groups: low (<90 eV) and high (≥90 eV). In Fig. 3, the blue dashed

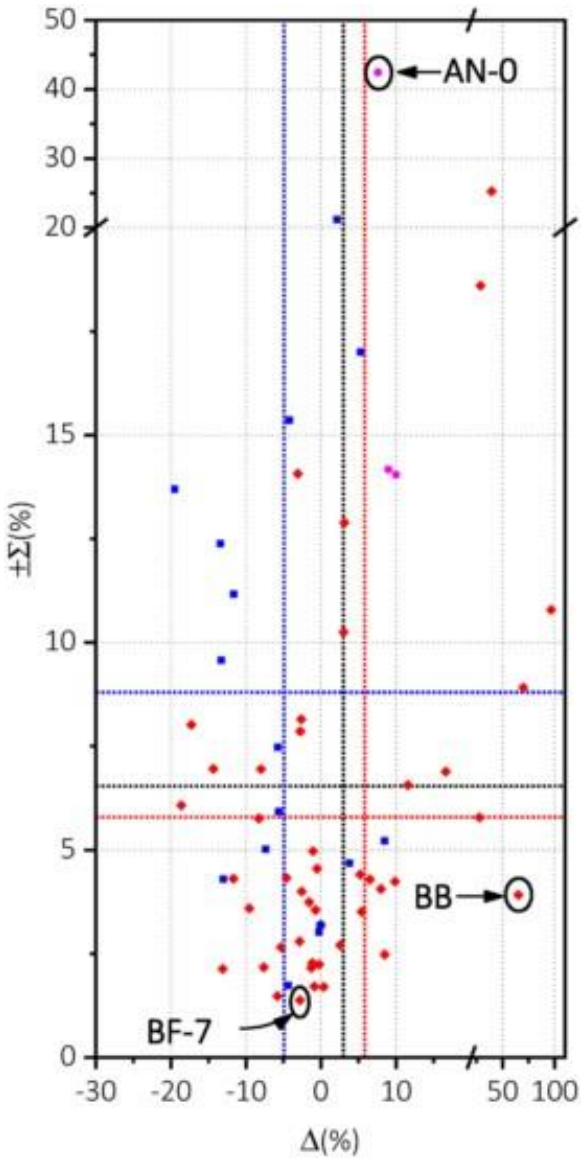

FIG. 3. Values of Δ (%) and ±Σ (%) for all the participants' datasets, where the red diamonds refer to high pass energy datasets (≥90 eV) and the blue squares refer to low pass energy datasets (<90 eV). The thick dashed lines show the average values of Δ (%) and ±Σ (%), shown in Table II, from all datasets (black central lines), high pass energy datasets (red lower horizontal and rightmost vertical), and low pass energy datasets (blue upper horizontal and leftmost vertical). The pink circles refer to datasets that have been replaced with newer data from the same participant and do not contribute to the average values of Δ (%) and ±Σ (%).

TABLE II. Average values of Δ (%) and Σ (%) for all participants' datasets, low pass energy datasets, and high pass energy datasets.

Dataset grouping	Δ (%)	Σ (%)
All participants	3.0%	±6.5%
Low pass energy (<90 eV)	−4.9%	±8.8%
High pass energy (≥90 eV)	5.8%	±5.7%

lines represent the mean value of Δ (%) and Σ (%) for datasets acquired at low pass energies, and the red dashed lines represent the mean value of Δ (%) and Σ (%) for datasets acquired at high pass energies. For low pass energies, the mean values of Δ (%) and Σ (%) are −4.9% and ±8.8%, respectively, and for high pass energies, the mean values are 5.8% and ±5.7%, respectively. The average results of Δ (%) and Σ (%) for low and high pass energies are reported in Table II.

The average offset remains within 10% for all the participants' datasets, as was similarly reported in the original NPL publication on LDPE calibration. However, from the point of view of obtaining correct relative intensities, the systematic deviation parameter is more important, and the effect of pass energies on Σ (%) is more pronounced. We observe that the lower pass energy group has more systematic deviation compared to the high pass energy. Increasing the analyzer pass energy increases the intensity of the photoelectron signal while sacrificing energy resolution, so in general we observe greater signal-to-noise across all kinetic energies in the high pass energy scans. The smaller signal-to-noise in the low count rate, low pass energy scans seems to result in more noise in the Q_{Au} and Q_{PE} values, which inevitably results in more variability in the fitting between T_{Au} and T_{PE}.

Three datapoints in Fig. 3 have been highlighted, which exhibit a large Σ (%) (AN-0), a large Δ (%) (BB), or both a low Σ (%) and Δ (%) (BF-7). The values of Q and T derived from LDPE and gold for these three datapoints are shown in Fig. 4 for demonstrative purposes. Similar figures have been produced for each set of the data submitted by the participants and can be viewed in the supplementary material (Sec. S2).[29] Participant AN-0 has produced a large Σ (%) due to large differences in the slope and shape between their T_{Au} and T_{PE}. Assuming a lack of operator error or sample issues such as contamination, this case is a cause for concern as the disparity between the LDPE and gold data could suggest an underlying issue with the spectrometer. Participant BB has produced a reasonable Σ (%) [in fact, better than the average Σ (%) for high pass energies], but there is a significant offset between T_{Au} and T_{PE} resulting in a large Δ (%). Although not ideal, this situation is workable as it still permits transmission function correction with an aim to extract relative peak intensities for quantification. The reason for the offset is also easier to diagnose; the most common cause for the offset between T_{Au} and T_{PE} is a difference in the x-ray source power, an insufficient warm up time for the x-ray source between the LDPE and gold scans, or failure to report data in counts per second. There is also supporting evidence to suggest that the topography of the LDPE after scraping with a scalpel can influence the absolute intensity of the LDPE spectrum (Fig. S8);[29] differences in Δ (%) up to 20% are possible through excessive scraping, but the sample orientation after scraping is not a critical factor. The small values of Δ (%) and Σ (%) obtained from participant BF-7 present a case where T_{Au} and T_{PE} are nearly identical, showing that, in the absence of instrumentation issues and operator error, the LDPE and gold intensity calibration methods can produce the same result.

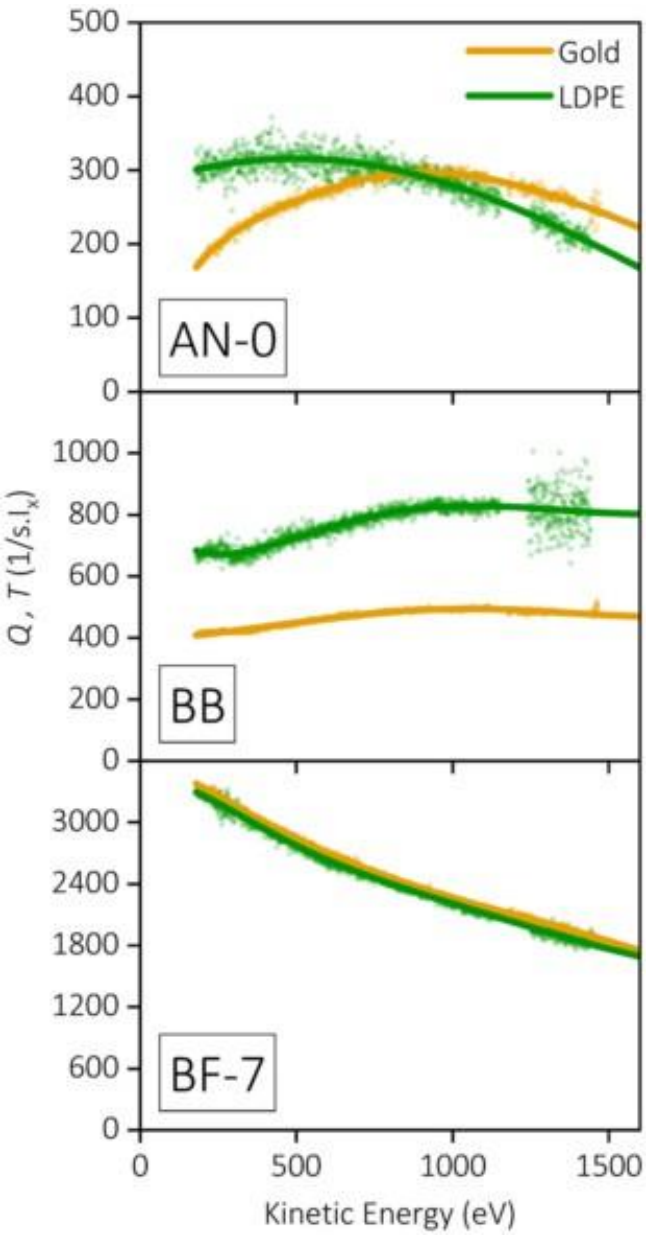

FIG. 4. Q (dots) and T (lines) calculated from LDPE and Au, respectively, for participants AN-0, BB, and BF-7, which have been highlighted in Fig. 3.

In the original protocol, participants were instructed to acquire a set of "dark noise" spectra with the x-ray source on and off. The average counts per second of this dark noise, D, would be subtracted from I_{PE}. This step is important, especially for the low count rate region on the low kinetic energy side of the C 1s peak. If the dark noise intensity is not removed from I_{PE}, then a significant intensity step is observed in Q_{PE} across the C 1s region, which cannot be fitted by the functional form of T_{PE}. In most cases, an instrument's dark noise will be constant across the entire kinetic energy range, and so dark noise correction is relatively straightforward. However, in the study, we encountered instances where the dark noise is dependent on the kinetic energy and needed to be given a functional form, D(E). Such a case is not ideal as it means that there is an underlying issue with the spectrometer. Figure 5(a) shows an example, from this VAMAS study (participant AX), of a spectrometer exhibiting a variable dark noise intensity. Assuming that the necessary troubleshooting has been attempted and D(E) is stable, then some arbitrary, noiseless function f(E) such as the one used in Fig. 5(a) can be used to fit D(E), which can then be used to perform the dark noise correction. It should be noted that the function f(E) is not a valid physical model describing the response of the spectrometer and only serves to correct the dark noise intensity. The effect of the variable dark noise correction on Q_{PE} (and, hence, T_{PE}) is shown in Fig. 5(b), where the LDPE intensity calibration method has been applied to I_{PE} with (i) constant D correction (black) and (ii) variable D(E) correction (red). In both cases, the values of Q_{PE} are similar on the low kinetic energy side of the C 1s region. However, in the case of constant dark noise correction, there is an intensity step in Q_{PE} over the C 1s region, which is caused by the mismatch of true dark noise intensity between the low and high kinetic energy regions. By using f(E) to correct the variable dark noise, the intensity mismatch around the C 1s region in Q_{PE} is drastically reduced, and the fitted T_{PE} more pertinently describes the shape of Q_{PE} between 1000 and 1500 eV, which accords more closely with T_{Au}. While the agreement between the resulting T_{PE} functions using different dark noise corrections is <1% at lower kinetic energies, there is a maximum difference of 4.9% at higher kinetic energies. This, therefore, demonstrates the importance of the correct subtraction of dark noise intensity from I_{PE}. While the variable dark noise correction is valid in this case, it should be stressed that such an issue with the spectrometer should be investigated prior to the calibration procedure.

Some participants' instruments exhibited behavior that could not be rectified within the scope of this interlaboratory study. In these cases, underlying instrument issues caused large deviations in Q, which could not be captured by the functional form for T. Figure 6 shows where unknown issues in participant BD's analyzer caused large deviations in Q_{PE} resulting in an intensity mismatch across the C 1s region. Furthermore, a significant loss of counts occurs in the low kinetic energy region (i.e., <300 eV) for both Q_{PE} and Q_{Au}. These features meant that the functional form of T could not converge on Q_{PE} and so the fitting failed. While not an ideal outcome, the low count rate of the LDPE spectrum clearly highlights an underlying issue with the spectrometer, which the gold spectrum did not pick up on. Hence, the LDPE intensity calibration method has potential as a tool to diagnose subtle issues in the analyzer, which manifest at low count rates.

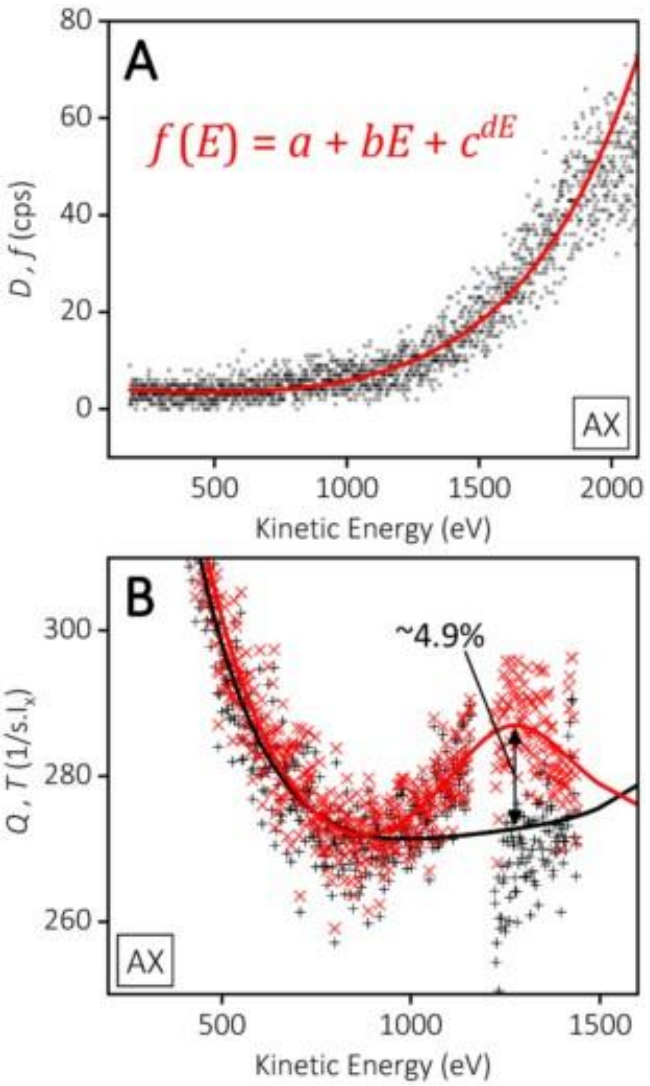

FIG. 5. (a) Variable dark noise D(E) recorded by participant AX (dots) fitted with an arbitrary function f(E) (line). (b) The effect of correcting D(E) shown by participant AX. The difference in Q_{PE} when corrected with a constant dark noise value (+) or f(E) (×). In the high kinetic energy, low count rate region above the C 1s, the difference in Q_{PE} is ~4.9%.

As previously mentioned, LDPE can be cleaned ex situ using nothing more than a clean scalpel or razor. It is important that the LDPE surface is scraped sufficiently to remove any surface oxidation or contamination, as obtaining meaningful values of Δ (%) and Σ (%) is highly dependent on acquiring both the LDPE and gold spectra under optimum conditions. Figure 7 demonstrates the effect of surface contamination on Q_{PE} and T_{PE}. The I_{PE} from participant AD-2 contained a significant O 1s peak and O KLL Auger feature, as well as smaller silicon and sulfur peaks (2p and 2s) in the HKE region. The inelastic background of the contaminant

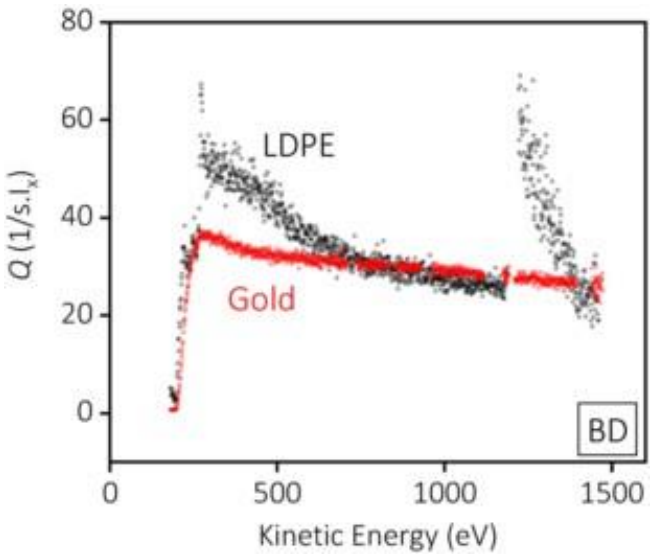

FIG. 6. Q_{PE} and Q_{Au} from participant BD showing significant internal scattering and intensity loss in the low kinetic energy region.

peaks is not accounted for by the LDPE reference spectrum and, thus, the resulting Q_{PE} contains peaks and inelastic background steps related to these elements. The increase in the inelastic background due to the silicon and sulfur peaks result in an intensity mismatch across the C 1s region, which T_{PE} cannot account for. The cumulative contributions of the background from the contamination peaks also result in a large deviation in Q_{PE} compared to

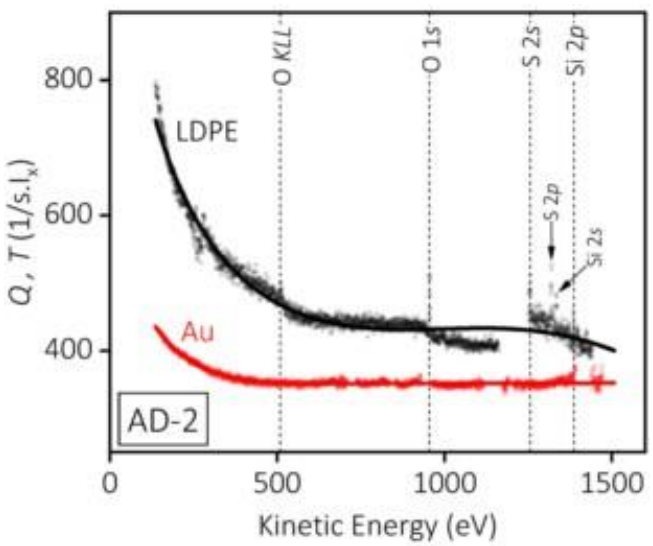

FIG. 7. Q_{PE} and Q_{Au} from participant AD-2 demonstrating the significant effect that contamination on the LDPE produces. Other elements (i.e., O, Si, and S) on the LDPE cause steps, discontinuities, and deviations in Q_{PE}.

Q_{Au} at low kinetic energies. Usually, this problem can be easily resolved by removing the LDPE sample from the XPS instrument and repeating the sample preparation step in the procedure. However, persistent contamination that cannot be removed may suggest either a bulk contaminated LDPE sample (requiring the LDPE to be replaced) or a contaminated XPS instrument (requiring a bakeout). Another source of contamination to consider is the scalpel or razor used in the LDPE preparation, for example, commercial razor blades often have a polytetrafluoroethylene coating, which could contaminate the LDPE surface with fluorine. In the case of gold, if there is any carbon contamination, this will cause a decrease in the count rate at lower kinetic energies due to the attenuation of the gold Auger features. Consequently, a significant deviation in Q_{Au} (and by extension, T_{Au}) at low kinetic energies will result in a similar low kinetic energy deviation in R_i when compared to data from a clean oxygen-free LDPE spectrum. It follows then that the values of Δ (%) and Σ (%) will not reflect a fair comparison, at least from a procedural perspective. Participant datasets with significant contamination on either the LDPE or gold have been identified in Table S2.[29]

In the VAMAS protocol, participants were instructed to obtain LDPE and gold spectra using the same analyzer settings and x-ray source power. However due to the orders-of-magnitude difference in photoelectron yield between these samples, acquisition settings that produce an appropriate signal-to-noise for the LDPE may result in detector saturation when measuring the gold.[27] Due to the order of the original protocol, it is probable that participants measured the LDPE first and then used the same parameters with the gold measurement, thus resulting in detector saturation. Some participants anticipated this issue and submitted gold spectra acquired using a lower x-ray anode emission current to avoid saturation. In this situation, a correction factor equal to the ratio of the differing x-ray anode emission currents is applied to I_{Au} or I_{PE} to reduce the x-ray power induced offset between Q_{Au} or Q_{PE}. Some participants' datasets exhibited evidence of detector nonlinearity as a result of detector saturation when measuring the gold. Figure 8(a) shows Q_{Au} and T_{Au} from participant AF. There is an uncharacteristic intensity increase around the low kinetic energy side of the gold peaks that T_{Au} does not fit correctly. The participant's gold spectrum recorded a maximum Au $4f_{7/2}$ count rate of ~1.95 Mcps and an average background count rate of ~340 kcps. In comparison, I_{PE} does not exhibit any evidence of detector saturation, and the maximum C 1s count rate was ~300 kcps. Figure 8(b) shows the measured intensity of I_{Au} plotted against the gold reference spectrum $I_{Au\text{-}ref}$ (geometry corrected) multiplied by T_{PE} (given that T_{PE} should not be affected by any nonlinearity arising from detector saturation). The red dots show the actual gold intensity recorded by the participant and the black line shows the expected gold intensity (which has a slope of ~1.12 to correct for the absolute offset between T_{Au} and T_{PE}). If the detector has a linear response, then we would expect the red dots and black line to agree, but we observe a clear detector nonlinearity in participant AF's data above ~300 kcps. Due to the low photoelectron yield from LDPE, nonlinearity effects are unlikely to occur during the calibration procedure, especially using standard acquisition parameters—regardless, the non-linear regime of the detector should be determined prior to calibration in order to be sure.

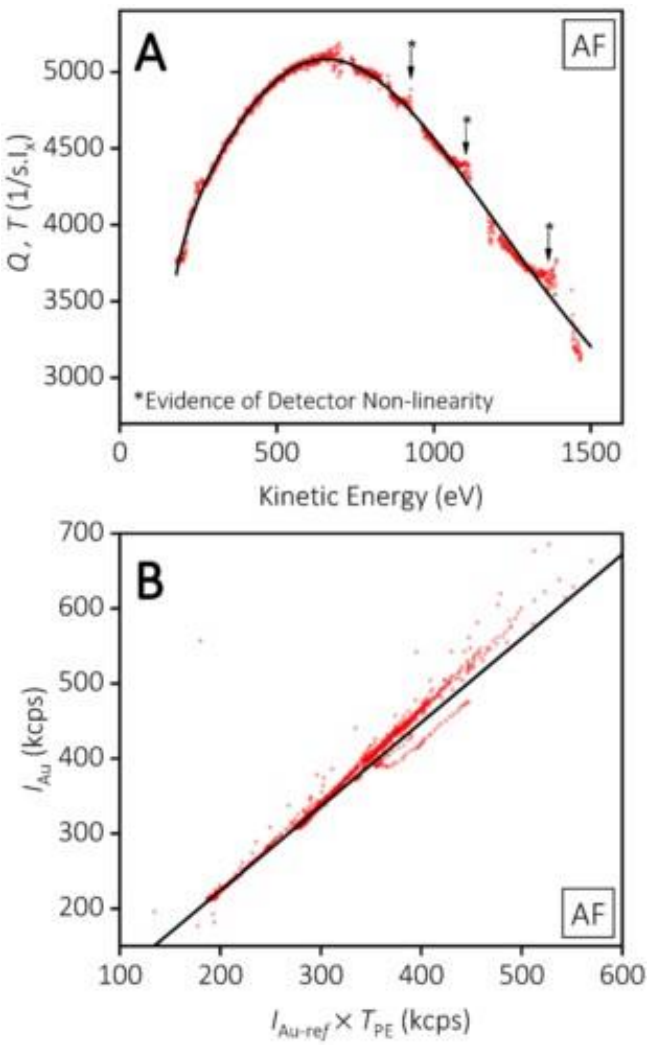

FIG. 8. (a) Q_{Au} (dots) and T_{Au} (line) from participant AF. The marked positions show an uncharacteristic increase in the spectrum intensity near the gold peaks, which may affect the fitting of T_{Au}. (b) Plotting the actual I_{Au} from participant AF (dots) against the expected $I_{Au\text{-}ref}$ (intensity corrected using T_{PE}, and corrected for average offset) (line) reveals detector nonlinearity above 300 kcps.

This work has demonstrated the huge variability between the transmission functions of XPS instruments from around the surface analysis community, in different laboratories, and using different commercial and home-built systems. At a minimum, it is important for XPS users to report the details of their instrument calibration, both in the energy and intensity scales, in their reports and publications in the interest of reproducibility.[28] However, we hope that this work has further communicated the vital need to use a consistent and traceable method of intensity calibration for the entire community of XPS users. This can be achieved via two avenues: (i) Table I shows that most of the participants are using commercial XPS systems, so it is probably reasonable to say that most of the surface analysis (and surface science) laboratories in the community are operating commercial systems as well. As of writing, XPS instrument manufacturers use their own in-house methods for intensity calibration, which may differ from company to company. An initial calibration is performed when the XPS instrument is sold, but this transmission function will quickly become redundant. If the user does not regularly calibrate their instrument, relying instead on the initial calibration file (assuming they are aware of it), then the results of their analyses will quickly become unreliable and irreproducible. An agreed traceable calibration method could be implemented by XPS instrument manufacturers and could either be integrated into both hardware and software allowing the user to easily and regularly calibrate the instrument or be provided as part of regular engineer servicing and maintenance. This effort could be underpinned by (ii) the publication of an international standard in collaboration with national metrology laboratories; As of writing, there is no international standard protocol for calibrating the intensity scale of XPS spectrometers. Such a standard should consider the alternative instrument configurations of its users, for example, some instruments do not have an in situ sputtering source for cleaning sample surfaces. The LDPE intensity calibration technique can contribute to such an international standard, allowing XPS users that do not have a sputter source to calibrate their instruments. Furthermore, it is a method that does not require noisy experimental reference spectra (the raw data from which would need to be stored in an accessible database), instead using a well-defined mathematical description that is applicable to all instrument geometries.[26]

Following the analysis of the interlaboratory study data and feedback from the participants, an improved calibration protocol using LDPE has been detailed in Sec. IV. This protocol addresses the issues brought up during the analysis with regard to geometry correction, variable dark noise correction, x-ray source warm up, sample contamination, analyzer internal scattering, and detector nonlinearity.

IV. XPS INTENSITY CALIBRATION PROTOCOL USING LDPE

The following intensity calibration protocol can be used for XPS instruments using a monochromatic Al Kα x-ray source and a low-energy electron source to neutralize surface charging. This protocol is applicable to instruments of any [a, b] geometry. This protocol requires a sample of high-purity LDPE and a clean scalpel or razor blade; N.B.: avoid using commercial razor blades, as they are typically coated in a lubricating fluorocarbon, which will contaminate the LDPE. It is advised that you read all the instructions carefully, ensuring that they are understood before continuing with the calibration procedure.

1. Determine the XPS instrument geometry, i.e., the source-to-analyzer angle "a," and the dihedral angle between the monochromator-sample-analyzer plane and the anode-monochromator-sample plane "b." See Shard and Reed.[26]
2. Mount a piece of LDPE onto a sample holder. A single piece of LDPE may be used for many calibrations if it has been stored in a cool and dark place, away from sources of fouling

(e.g., solvent fumes, heat, damp, prolonged light exposure, etc.). If the LDPE shows any sign of contamination or fouling, replace the LDPE stock with new material.

3. Using a clean scalpel or razor blade, firmly scrape the surface of the LDPE several times until the surface turns from shiny to matte in appearance. Do not overscrape the LDPE; we recommend no more than ten scrapes for a given area.
4. Immediately place the LDPE into the instrument load lock, and pump down. As soon as possible, transfer the LDPE sample into the analysis chamber.
5. With the LDPE sample positioned away from the analysis position, acquire a survey spectrum between 180 and 1500 eV kinetic energy to determine the "x rays OFF dark noise."
6. Switch on the x-ray source and wait at least 30 min for the source to equilibrate. Some older or aging instruments may require longer.
7. With the LDPE sample positioned away from the analysis position, acquire a survey spectrum between 180 and 1500 eV kinetic energy to determine the "x rays ON dark noise." Compare the dark noise surveys and ensure that they have a constant intensity across the entire spectrum range. If the dark noise varies across the survey range, this may be indicative of an instrument issue that should be investigated. As a temporary approach, prior to the instrument being fixed, if the dark noise intensity follows a predictable and stable pattern, a suitable function D(E) may be fitted to the dark noise intensity, which can then be used.
8. Move the LDPE into the analysis position. Optimize the sample-to-analyzer distance and the charge compensation settings to maximize the C 1s intensity. Ensure that the C 1s is a single peak positioned between 1201 and 1206 eV kinetic energy.
9. Acquire a survey spectrum between 180 and 1500 eV kinetic energy using a high pass energy (i.e., ≥90 eV). Ensure that no elements other than carbon are detected. If other elements are detected, move around the LDPE surface to find a contaminant-free area. If unsuccessful, remove the LDPE from the XPS instrument and start the calibration protocol again from step 3. If this fails again, check the LDPE, scalpel, laboratory, and XPS instrument for sources of surface contamination. If necessary, use a fresh piece of LDPE.
10. Change the spectrometer settings to the mode that requires calibration (i.e., pass energy, lens mode, exit and entrance slit, etc.) and allow enough time for the instrument to equilibrate if required. From this point forward, use the same acquisition parameters for all scans unless stated otherwise. Do NOT switch the x-ray source off between scans.
11. Acquire a survey spectrum between 180 and 1500 eV kinetic energy, E. Designate this spectrum $I_{initial}(E)$.
12. Acquire a survey spectrum between 1195 and 1500 eV kinetic energy with an acquisition time ~30 to 40 times longer than $I_{initial}(E)$. This can be done by either increasing the dwell time per step or increasing the number of acquisitions/sweeps/repetitions. Take an average of all spectra acquired in the HKE region in counts per second. (N.B.; averaging XPS spectra needs to be done in counts per second, your acquisition may automatically do this). Designate this spectrum $I_{HKE}(E)$ (where HKE is "high kinetic energy").
13. Acquire a survey spectrum between 180 and 1500 eV kinetic energy. Designate this spectrum $I_{HKE}(E)$.
14. Export the $I_{initial}(E)$, $I_{HKE}(E)$, and $I_{final}(E)$ spectra in counts per second and plot them. All three spectra should overlap and have no significant differences in intensity. Also ensure that these spectra have not been intensity calibrated automatically by the acquisition software. Divide $I_{final}(E)$ by $I_{initial}(E)$ and ensure that the ratio is unity across the entire kinetic energy range—if the ratio does not equal unity, then this could indicate an issue with the instrument (sloped ratio) or simply that the x-ray source has not sufficiently equilibrated (offset).
15. Repeat steps 10-14 for each of the usual operating modes of the instrument (i.e., pass energies, lens modes, slit/iris settings, etc.).
16. For each operating mode, combine the corresponding $I_{initial}(E)$, $I_{HKE}(E)$, and $I_{final}(E)$ spectra into a single spectrum in counts per second and subtract the average intensity in counts per second above the photon energy D to account for dark noise [or subtract D(E) if variable dark noise was observed in step 7]. The combined spectrum $I_{PE}(E)$ is described mathematically as

$$I_{PE}(E) = \begin{cases} (I_{initial}(E) + I_{final}(E))/2 - D(E), & E < 1195\ \text{eV} \\ I_{HKE}(E) - D(E), & E \geq 1195\ \text{eV} \end{cases} \quad (4)$$

17. For each operating mode, calculate the LDPE reference spectrum[26] $I_{ref}(E)$ for the relevant instrument geometry [a, b] with the adjustable variable q, which is the kinetic energy offset between $I_{PE}(E)$ and $I_{ref}(E)$.
18. For each operating mode, divide $I_{PE}(E)$ by $I_{ref}(E)$ and adjust q to eliminate sharp features at the C KLL edge (E ~ 280 eV). The resulting ratio gives $Q_{PE}(E)$ from which datapoints between 1150 and 1220 eV kinetic energy and values greater than 1440 eV should be removed.
19. Check $Q_{PE}(E)$ for any issues before continuing, such as intensity steps over the C 1s region, sharp features in the data, uncharacteristic intensity increases near C 1s or C KLL, etc. These features could indicate either an issue with the data acquisition (e.g., contaminated LDPE, accidental export of an instrument's old T, etc.) or an issue with the spectrometer (e.g., internal scattering, detector saturation, etc.). Investigate these issues before continuing, and if necessary, start the calibration procedure again (from step 3).
20. For each operating mode, use power law fits (see S1)[29] in the regions within ~100 eV from the ends of $Q_{PE}(E)$ (i.e., ~180 to 280 eV and ~1340 to 1440 eV). Using the power law fits, extrapolate $Q_{PE}(E)$ below 180 eV (to ~100 eV) and above 1440 eV (to ~2000 eV). About ten datapoints above and below the limits of $Q_{PE}(E)$ is enough. This ensures that the subsequent fitting does not drastically diverge beyond the limits of $Q_{PE}(E)$.
21. For each operating mode, fit $Q_{PE}(E)$ with a functional form [Eq. (2) from Ref. 22] to obtain the transmission function $T_{PE}(E)$.
22. The transmission function $T_{PE}(E)$ may be used to intensity correct spectra acquired using the same operating parameters: To correct the full spectrum, the intensity at each energy E is divided by $T_{PE}(E)$; this method is necessary if inelastic

background analysis is intended. To correct peak areas, the peak area and peak energy, E_P, are evaluated in the raw data

and the peak area divided by $T_{PE}(E_P)$ prior to the application of sensitivity factors or other types of analysis.

V. CONCLUSIONS

The results of this interlaboratory study have shown that the LDPE calibration method can provide an accurate transmission function that agrees with the more established NPL calibration method. Except for two submitted datasets (due to spectrometer issues), every participant's LDPE spectra could be used to determine the function T for their spectrometer, therefore highlighting the usability and validity of the LDPE intensity calibration method across different laboratories and XPS instruments. We note that the high pass energy datasets result in less systematic deviation compared to the low pass energy datasets, that is, ±5.7% for high pass energies and ±8.8% for low pass energies. In short, this is due to a difference in the intensities of the acquired I_{PE}; the high pass energy datasets have a greater signal-to-noise and are less affected by errors in determining the dark noise contribution. In practice, most XPS users will only require an accurate transmission function for their high pass energy acquisition parameters, which will be used to obtain atomic compositions from a survey scan. If the transmission function does not greatly vary over the energy range of the calibration, then the analyzer response over a smaller range, such as over a single core level, may be ignored for the purposes of a standalone peak fit. The larger systematic deviation at low pass energies may be reduced by increasing the acquisition time to improve signal-to-noise, although the Q_{PE} will still be highly sensitive to any dark noise contribution. The interlaboratory study has also highlighted some advantages and disadvantages to the method in addition to those discussed at the beginning of this article, i.e., ex situ sample preparation without an Ar-ion sputter source, insensitive to carbon contamination and simple mathematically generated reference spectra. A continuous noise-free reference spectrum for LDPE can now be generated for any quartz-monochromated Al Kα instrument in the [a, b] geometry. The photoelectron yield from LDPE is low, which means that that long acquisition times are required to obtain a suitable signal-to-noise, especially in the HKE region above the C 1s peak. However, this means that LDPE is very unlikely to saturate the detector and cause nonlinearity effects in the spectrum even at high x-ray powers, which is an issue that can arise when calibrating with metals like gold, silver, and copper. This means that the operator can calibrate their instrument using their normal acquisition parameters and x-ray source power. The low intensity of the LDPE spectrum means that it is more sensitive to underlying spectrometer issues such as low-level internal scattering or variable dark noise, as these can prevent the fitting of an appropriate T. However, this also means that the LDPE intensity calibration method can potentially be used to diagnose issues with the spectrometer, which may be missed when using gold, silver, or copper as the reference material. With these attributes in mind, LDPE appears to be a suitable candidate as a secondary reference material for XPS intensity calibration and could contribute to the formulation of an international standard as an alternative calibration method.

ACKNOWLEDGMENTS

We acknowledge funding from the project National Measurement System by the UK Department for Business, Energy and Industrial Strategy (No. NMS/ST20). We thank the chair of VAMAS TWA 2, Ian Gilmore, and Charles Clifford for their help initiating the interlaboratory study. We also sincerely thank all the participants of the VAMAS A27 interlaboratory study; A.P.B. would like to acknowledge that a portion of this research was conducted at the Center for Nanophase Materials Sciences, which is a DOE Office of Science User Facility; D.G.C. gratefully acknowledges support from the U.S. National Institutes of Health (Grant No. EB-002027); E.F.S. would like to acknowledge the EPSRC grant for the Kratos LiPPS XPS instrument (No. EP/K005138/1).

DATA AVAILABILITY

The data that support the findings of this study are available from the corresponding author upon reasonable request.

REFERENCES

[1]C. J. Powell, Microsc. Today 24, 16 (2016).
[2]A. Jablonski and C. J. Powell, Surf. Sci. Rep. 47, 33 (2002).
[3]V. I. Nefedov and I. S. Nefedova, J. Electron Spectrosc. 107, 131 (2000).
[4]J. J. Yeh and I. Lindau, Atom. Data Nucl. Data 32, 1 (1985). [5]J. H. Scofield, J. Electron Spectrosc. 8, 129 (1976).
[6]M. Baker, Nature 533, 353 (2016).
[7]D. R. Baer and M. H. Engelhard, J. Surf. Anal. 26, 94 (2019).
[8]M. R. Linford et al., Microsc. Microanal. 26, 1 (2020).
[9]International Organization for Standardization, ISO 15472:2010—Surface Chemical Analysis—X-ray Photoelectron Spectrometers—Calibration of Energy Scales (International Organization for Standardization, Geneva, 2010).
[10]International Organization for Standardization, ISO 24237:2005—Surface Chemical Analysis—X-ray Photoelectron Spectroscopy—Repeatability and Constancy of Intensity Scale (International Organization for Standardization, Geneva, 2005).
[11]L. T. Weng, G. Vereecke, M. J. Genet, P. Bertrand, and W. E. E. Stone, Surf. Interface Anal. 20, 179 (1993).
[12]R. Hesse, P. Streubel, and R. Szargan, Surf. Interface Anal. 37, 589 (2005).
[13]R. C. Wicks and N. J. C. Ingle, Rev. Sci. Instrum. 80, 053108 (2009).
[14]J. Trigueiro, W. Lima, N. Bundaleski, and O. M. N. D. Teodoro, J. Electron Spectrosc. 222, 122 (2018).
[15]B. Gruzza, P. Bondot, A. Porte, C. Jardin, and G. Gergely, Acta Phys. Pol. A 81, 159 (1992).
[16]C. S. Hemminger, T. A. Land, A. Christie, and J. C. Hemminger, Surf. Interface Anal. 15, 323 (1990).
[17]J. Osterwalder, M. Sagurton, P. J. Orders, C. S. Fadley, B. D. Hermsmeier, and D. J. Friedman, J. Electron Spectrosc. 48, 55 (1989).
[18]M. Holzweber, A. Lippitz, R. Hesse, R. Denecke, W. S. M. Werner, and W. E. S. Unger, J. Electron Spectrosc. 233, 51 (2019).
[19]M. P. Seah, J. Electron Spectrosc. 71, 191 (1995).
[20]M. P. Seah, Surf. Interface Anal. 20, 243 (1993).
[21]M. P. Seah and G. C. Smith, Surf. Interface Anal. 15, 751 (1990).
[22]A. G. Shard and S. J. Spencer, Surf. Interface Anal. 51, 618 (2019).
[23]A. G. Shard, Surf. Interface Anal. 46, 175 (2014).
[24]B. P. Reed, S. J. Spencer, and A. G. Shard, "VAMAS TWA 2, 2019, sub-project A27—Intensity calibration for XPS instruments using low-density poly(ethylene)—protocol for analysis," NPL Report AS 100, National Physical Laboratory, Teddington, UK, 2019.
[25]A. Herrera-Gomez, J. Electron Spectrosc. 182, 81 (2010).
[26]A. G. Shard and B. P. Reed, J. Vac. Sci. technol. A 38, 063209 (2020).

[27] M. P. Seah, I. S. Gilmore, and S. J. Spencer, J. Electron Spectrosc. 104, 73 (1999).
[28] A. G. Shard, J. Vac. Sci. Technol. A 38, 041201 (2020).
[29] See supplementary material at https://doi.org/10.1116/6.0000577 for (S1) Protocol for VAMAS interlaboratory study circulated to participants; (S2) Table showing important experimental information, percentage values of Δ (%) and Σ (%), and comments which describe issues or observations with the participants' datasets or direct feedback from the participants; (S2 continued) Figures showing participants' transmission functions calculated from LDPE and gold; (S3) Supporting figures including: a graphical representation of R_i, Δ, and Σ from Eqs. (2) and (3); and transmission functions calculated at NPL using LDPE prepared with differing surface topographies.